JLB

Article

CCRL2 regulates M1/M2 polarization during EAE recovery phase

Cristina Mazzon,[*,†,1] Lucia Zanotti,[†,1] Li Wang,[†,1,2] Annalisa Del Prete,*[*,†,1] Elena Fontana,* Valentina Salvi,* Pietro Luigi Poliani,* and Silvano Sozzani*[*,†,3]

*Department of Molecular and Translational Medicine, University of Brescia, Italy; and †Humanitas Clinical and Research Center, Rozzano, Italy

RECEIVED SEPTEMBER 28, 2015; REVISED DECEMBER 22, 2015; ACCEPTED DECEMBER 23, 2015. DOI: 10.1189/jlb.3MA0915-444RR

ABSTRACT

Chemokine (CC motif) receptor-like 2 is a 7-transmembrane protein related to the family of the atypical chemokine receptors, which are proteins devoid of chemotactic activity and involved in the control of inflammation. Experimental autoimmune encephalitis is an autoimmune disorder that replicates the inflammatory aspects of multiple sclerosis. Chemokine (CC motif) receptor-like 2–deficient mice developed exacerbated, nonresolving disease with protracted inflammatory response and increased demyelination. The increased severity of the disease was associated with higher levels of microglia/macrophage activation markers and imbalanced M1/M2 polarization. Thus, chemokine (CC motif) receptor-like 2 is involved in the downregulation of central nervous system–associated experimental autoimmune encephalitis inflammation in the recovery phase of the disease. Therefore chemokine (CC motif) receptor-like 2 should be considered to be a molecule involved in the regulation of the inflammatory response associated with multiple sclerosis. *J. Leukoc. Biol.* 99: 1027–1033; 2016.

Introduction

EAE is an autoimmune disorder that models the inflammatory aspects of MS [1, 2], a chronic immune-mediated demyelinating disease of the CNS of unknown origin [3].

EAE is characterized by leukocyte recruitment and activation in the CNS, and the number of infiltrated macrophages has been shown to correlate with disease severity [4]. The inflammatory infiltrate represents the main target of the therapies currently available for MS [5].

Chemotactic factors constitute a heterogeneous family of agonists that interact with G-protein-coupled 7-transmembrane domain receptors [6, 7]. Chemokines and their cognate receptors represent the main family of chemotactic proteins, and several lines of evidence demonstrate their key role as functional mediators in the pathologic outcome of EAE [8]. Chemotactic proteins can also bind a subfamily of receptors referred to as ACKRs which lack chemotactic activity and are believed to limit inflammation [6, 9]. Previous work showed that ACKR3, a member of the ACKR family, plays a role in CNS physiopathology, acting as a critical chemokine scavenger in brain microvessel endothelium [10].

CCRL2 is a 7-transmembrane protein that shares many characteristics with the ACKRs, including the lack of certain consensus sequences and of the ability to induce functional responses [6, 9]. CCRL2 was originally described as an LPS-inducible gene in the mouse macrophage cell line RAW264 [11]. CCRL2 is expressed by most leukocyte subsets, including activated monocyte/macrophages, neutrophils, dendritic cells, lymphocytes, NK cells, mast cells, and $CD34^+$ precursors and by vascular and lymphatic endothelium [12–17]. CCRL2 has been shown to be upregulated in vitro and in vivo in mouse microglia and astrocytes and to be expressed in EAE by infiltrating macrophages [18, 19]. In addition, a nonredundant role for CCRL2 has been proposed in dendritic cell trafficking and in the control of airway inflammatory reactions [20]. CCRL2 binds chemerin, a chemotactic protein that also binds ChemR23 a functional chemotactic receptor expressed by APCs, such as macrophages, dendritic cells, and microglia [21–23]. In this study we investigated the role of CCRL2 in a model of EAE. The results showed that CCRL2 plays an unexpected anti-inflammatory role during the chronic phase of the disease.

MATERIALS AND METHODS

Mice

Age-matched female 8- to 12-wk-old mice were used in all EAE experiments. CCRL2 KO mice (on C57BL/6 background) were obtained as described [20]

Abbreviations: ACKR = atypical chemokine receptor, CCRL2 = chemokine (CC motif) receptor-like 2, d.p.i. = days after immunization, EAE = experimental autoimmune encephalitis, KO = knockout, MBP = myelin basic protein, MOG = myelin oligodendrocyte glycoprotein, MS = multiple sclerosis, PFA = paraformaldehyde, qPCR = quantitative polymerase chain reaction, TREM = triggering receptor expressed on myeloid cells, WT = wild-type

1. These authors contributed equally to this work.
2. Current affiliation: Department of Immunology and Microbiology, Shanghai Jiao Tong University School of Medicine, Shanghai, China
3. Correspondence: Silvano Sozzani, Department of Molecular and Translational Medicine, University of Brescia, Viale Europa 11, 25123 Brescia, Italy, E-mail: silvano.sozzani@unibs.it

0741-5400/16/0099-1027 © Society for Leukocyte Biology

and bred at the Charles River animal facility (Calco, Italy). Procedures involving animals and their care conformed to institutional guidelines in compliance with national (D.L. N.26, 4-3-2014) and international (Directive 2010/63/EU revising Directive 86/609/EEC on the protection of animals used for scientific purposes, as adopted on September 22, 2010) law and policies. The study was approved by the Italian Ministry of Health.

EAE induction

WT C57BL/6 and CCRL2 KO mice were immunized by subcutaneous injection into the side flanks of 100 μg $MOG_{aa35–55}$ (MEVGWYRSPFSRVVHLYRNGK, AnaSpec, Inc., Fremont, CA, USA), in IFA (Thermo Scientific-Gibco, Grand Island, NY, USA) containing 400 μg of heat-inactivated *Mycobacterium tuberculosis* H37 RA (BD Biosciences-Difco, San Jose, CA, USA). The mice received 2 i.v. injections of 350 ng pertussis toxin (List Biologic Laboratories, Inc., Campbell, CA, USA) on d 0 and +2 after immunization. Onset and progression of EAE symptoms were monitored daily with a standard clinical scale ranging from 0 to 5 [2, 24]. The disease incidence was defined as the percentage of mice that displayed any clinical signs of disease. Disease onset was defined as the first day of 2 consecutive days with a clinical score.

CNS-infiltrating mononuclear cell purification

Anesthetized mice were perfused through the left cardiac ventricle with cold PBS. The brain and spinal cord were dissected. Brain tissue was dissociated and digested according to a published protocol [25]. Single-cell suspensions were resuspended in 35% Percoll (GE Life Sciences, Pittsburgh, PA, USA) and deposited on 70% Percoll. After a 30-min centrifugation at 2500 rpm at 4°C, mononuclear cells were isolated from the interphase of 35/70% isotonic Percoll gradient, washed twice in medium, and used for further RT-PCR and FACS analysis.

qPCR

Real-time qPCR was performed on an ABI 7900HT Fast Real-time PCR system (Thermo Scientific-Applied Biosystems, Foster City, CA, USA) with SYBR Green PCR Master Mix system (Thermo Scientific-Applied Biosystems).

Histology and immunohistochemistry

Mice were perfused with PBS and 4% PFA. Brains and spinal cords were harvested, and tissues were fixed overnight in 4% PFA before paraffin embedding. Consecutive 2 μm-thick sections were taken, and routine H&E staining were analyzed by 2 authors (E.F., P.L.P.) in a blind protocol, to assess basic histopathological changes. Immunohistochemistry and morphometric analysis were performed as described [26]. The following polyclonal and monoclonal primary antibodies were used: rabbit anti-CD3 (1:100; Thermo-Scientific, Carlsbad, CA, USA), rabbit anti-Iba-1 (1:300; Wako, Osaka, Japan), rabbit anti-IL-1β (1:200; Santa Cruz Biotechnology, Dallas, TX, USA), rabbit anti-Ym1 (1:200, StemCell Technologies, Vancouver, BC, Canada), rabbit anti-glial fibrillary acidic protein (1:200; Dako, Carpinteria, CA, USA), and rat anti-MBP (1:50; Chemicon, Temecula, CA, USA). Digital images were acquired by a DP70 camera mounted on a Bx60 microscope (Olympus, Tokyo, Japan), with $Cell^F$ Imaging software (Soft Imaging System GmbH, Münster, Germany). The degree of inflammation is expressed as the percentage of infiltrated area vs. the total spinal cord section, and demyelination was evaluated by measuring the percentage of the demyelinated area vs. the total white matter area in each spinal cord section. An average of 8–10 spinal cord sections was evaluated for each mouse. Macrophages and microglia were discriminated based on their morphology [27], and cell infiltration and activation were evaluated by assigning a semiquantitative score to Iba-1 immunostaining and grading as follows: 0, none; 1, low; 2, moderate; and 3, high.

Statistical analysis

Statistical significance was calculated by Student *t* test, Mann-Whitney *U* test, and 1-way ANOVA, as appropriate.

RESULTS

CCRL2 expression by CNS mononuclear cells parallels the development of EAE

CCRL2 expression was evaluated by qPCR in mononuclear cells isolated from the CNS of mice in the $MOG_{aa35–55}$ model of EAE [2, 24]. Figure 1A shows that CCRL2 mRNA was barely detectable in cells from untreated WT animals, but was induced by immunization at time points that preceded the appearance of clinical signs (8 d.p.i.; 4.3-fold). CCRL2 mRNA expression further increased at the peak phase of the disease (20 d.p.i.; 16.6-fold) and started to decline thereafter (36 d.p.i.). As expected, no expression of CCRL2 mRNA was detected in KO mice (data not shown). Conversely, the expression of ChemR23 was already detectable in the basal condition and paralleled the development of the disease. At the peak of disease (20 d.p.i.) and thereafter (36 d.p.i.), the expression of ChemR23 in CCRL2 KO was more pronounced than in WT mice (Fig. 1B).

CCRL2 KO mice show exacerbated EAE clinical and histopathological signs

The classic neurologic deficit of EAE (ascending paralysis) appeared both in WT and CCRL2 KO mice at ~12 d.p.i., with a similar incidence. However, CCRL2 KO mice showed a statistically significant increase in severity compared with that in WT animals, thus supporting a functional role for CCRL2 in the pathogenesis of the disease (**Fig. 2**). No statistically significant difference was present in the day of onset or in the incidence of the disease between the 2 experimental groups. An increased EAE clinical score was observed in CCRL2 KO mice from the time of the peak through the recovery phase. Consistent with these observations, CCRL2 KO mice presented significantly increased mortality, higher maximum clinical score, and greater cumulative disease score (**Table 1**).

Histopathological examination of spinal cords showed neuropathological features that correlated with the increased clinical score observed in CCRL2 KO mice. At 16 d.p.i. H&E staining revealed a similar degree of leukocyte infiltration between KO and WT mice, preferentially distributed along the meninges and the perivascular areas (data not shown). However, during the recovery phase (33 d.p.i.) the extent of the infiltrated area was

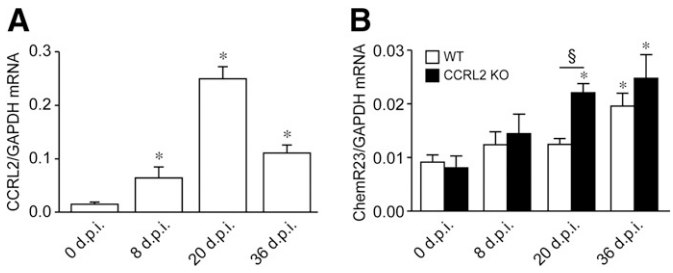


Figure 1. CCRL2 is up-regulated in CNS mononuclear cells during EAE. Mononuclear cells were isolated from CNS by Percoll fractionation at the indicated time points. Total RNA was then purified and subsequently analyzed by qRT-PCR. Results were normalized to the expression of a housekeeping gene (*GAPDH*). Data are the mean ± SEM of results in 5–6 mice per group and represent 1 of 3 independent experiments. $^*P < 0.05$, WT or CCRL2 KO mice vs. respective basal control group (0 dpi); $^§P < 0.05$, WT vs. CCRL2 KO mice.

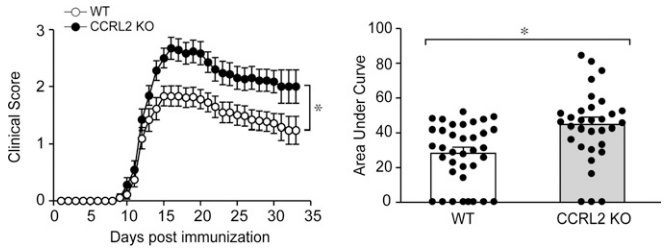


Figure 2. CCRL2 KO mice develop exacerbated EAE. WT and CCRL2 KO mice were subcutaneously immunized by injection into the side flank of 100 μg $MOG_{aa35–55}$ containing 400 μg heat-inactivated *M. tuberculosis*. Mice received 2 i.v. injections of 350 ng pertussis toxin on d 0 and 2 after immunization. Left: mean disease scores ± SEM of WT and CCRL2 KO mice evaluated daily after EAE induction. Right: the average score of the area under the curve of 3 independent experiments (± SEM) calculated from the EAE clinical score (0–33 d.p.i.). $*P < 0.05$, WT vs. CCRL2 KO mice.

significantly higher in CCRL2 KO mice (**Fig. 3A**, insets). The more severe clinical situation, observed in KO mice, was mirrored by increased myelin loss (Fig. 3B). Glial fibrillary acidic protein immunostaining highlighted a diffuse and intense gliosis in WT spinal cords, along with a significant depletion of inflammatory cells. In contrast, in CCRL2 KO mice, the exuberant inflammatory reaction was associated with only mild gliosis (data not shown). Taking together, these findings show that the absence of CCRL2 causes an exacerbation and persistence of the disease during the recovery phase.

CCRL2 KO mice do not show altered T cell priming after $MOGaa_{35–55}$ immunization

Because EAE is a $CD4^+$ T cell-mediated demyelinating disease of the CNS [1, 2], it was of interest to investigate whether the absence of CCRL2 would influence the proliferation and priming of encephalitogenic T cells. Therefore, cell proliferation and cytokine secretion were evaluated after $MOG_{aa35–55}$ stimulation of cells obtained from immunized WT and CCRL2 KO mice. In vitro stimulation of CCRL2 KO inguinal, brachial, and cervical lymph node cell suspensions, collected at 10 d.p.i., did not show any significant difference in the proliferation index compared to that of the WT counterpart (**Fig. 4A**). Likewise, CCRL2 KO cells obtained from inguinal and brachial lymph nodes produced similar levels of IFNγ in response to the different $MOG_{aa35–55}$ peptide concentrations. Cells obtained from cervical lymph nodes showed a tendency to produce lower levels of IFNγ, although the results did not reach statistical significance (Fig. 4B). Consistent with these results, adoptive transfer of $MOG_{aa35–55}$-reactive lymphocytes obtained from immunized mice into WT and CCRL2 KO recipients produced EAE with similar frequency and severity, independent of the strain source of the transferred cells or the recipient mice. Finally, no significant difference was observed in the frequency and the absolute number of $CD4^+Foxp3^+$ regulatory T cells, in the preclinical (8 d.p.i.) and clinical (20–36 d.p.i.) phases of the disease (data not shown).

CCRL2 KO mice show altered polarization in CNS-infiltrating T cells during EAE

The expression of the T cell-polarizing transcription factors T-bet (Th1), RORγT (Th17), and GATA-3 (Th2) was also investigated in cells purified from the CNS during EAE. Figure 5 shows that T-bet and GATA-3 expression were maximum at the peak phase of the disease (20 d.p.i.) and started to decline thereafter (36 d.p.i.). However, significant differences were observed between the 2 experimental groups, with T-bet being more highly expressed in CCRL2 KO mice at 20 d.p.i., and GATA-3 being much more highly expressed in WT mice during the remission phase, at 36 d.p.i. In one experiment, the increase in Th1-polarized T cells in CCRL2 KO mice was also detected as an increase in percentage of $CD4^+IFN\gamma^+$ cells in CNS-infiltrating cells at 20 d.p.i. (data not shown). Conversely, no difference in RORγT expression was observed between the 2 groups. These results are consistent with the exacerbation of the inflammation and the defective recovery phase observed in KO mice (Fig. 5).

CCRL2 KO mice show altered macrophage/microglia M1/M2 balance during the EAE recovery phase

Microglia and macrophages actively participate in EAE pathogenesis and progression [28], assuming different functional states in relation to the nature of the local microenvironment [29]. qRT-PCR, performed with mRNA isolated from purified CNS mononuclear cells, showed that the microglia and macrophage activation markers Iba-1 and CD68 were increased in CCRL2 KO mice, compared with those WT mice in all kinetic aspects investigated (**Fig. 6A**). Recently, TREM2 was described as a new microglia activation marker involved in the response to

TABLE 1. Onset and progression of EAE symptoms

Group	Disease incidence (%)	Mortality (%)	Disease onset	Maximum clinical score	Cumulative disease score
WT ($n = 36$)	77.7	0.00	12.18 ± 0.27	2.52 ± 007	28.70 ± 3.04
CCRL2 KO ($n = 32$)	90.6	12.23*	11.76 ± 0.24	3.25 ± 0.15*	45.03 ± 3.76*

Symptoms were monitored daily according to a standard clinical scale ranging from 0 to 5, as follows: 0, asymptomatic; 1, limp tail; 2, limp tail and hind limb weakness; 3, partial hind limb paralysis; 4, complete hind limb paralysis; and 5, moribund state/death [24]. Disease onset was defined as the first day of 2 consecutive days with a clinical score. Disease incidence was defined as the percentage of mice that displayed any clinical sign of disease. Cumulative disease and maximum clinical scores were calculated as described [24]. $*P < 0.05$, WT vs. CCRL2 KO mice.

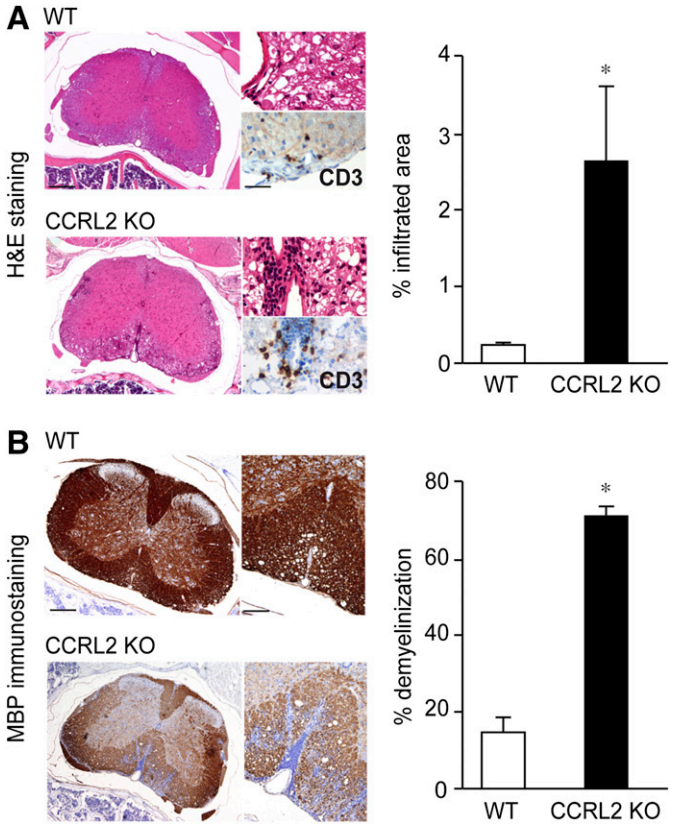


Figure 3. CCRL2 KO mice present increased demyelination and inflammation during the EAE recovery phase. Mice were euthanized during the recovery phase (at 33 d.p.i.), and CNS tissues were subjected to histopathological analysis. An average of 8–10 spinal cord sections for each mouse was evaluated. (A) Left: representative sections of lumbar spinal cord from WT and CCRL2 KO mice with clinical signs of EAE stained with H&E. Top insets: magnification of H&E-stained tissue. Original magnification: ×4; insets ×40. Bottom insets: CD3 staining of T cell infiltration. Magnification, ×40. Right: the degree of inflammation, expressed as a percentage of infiltrated area over the total spinal cord section. (B) Left: representative sections of WT and CCRL2 KO spinal cords stained with antibodies to MBP. Magnification: ×4, left; ×20, right. Demyelination was evaluated as a percentage of the total white matter area for each spinal cord section. Right: the demyelination analysis on sections scored in a blinded manner ($n = 5$ for WT; $n = 6$ for CCRL2 KO). *$P < 0.05$.

tissue damage [27, 30]. TREM2 mRNA was already increased in CCRL2 KO in the preonset phase of the disease (8 d.p.i.) and was further increased at the peak and during the recovery phase, compared to WT mice. Immunohistochemistry analysis was performed at the peak of disease (16 d.p.i.) and during the recovery phase (33 d.p.i.). WT and CCRL2 KO mice showed a similar distribution of myeloid cells in the CNS sections analyzed. However, a clear increase in the number of Iba-1$^+$ cells (both microglia and macrophages) was observed in CCRL2 KO mice at 33 d.p.i. (Fig. 6B).

The M1 and M2 polarization state was investigated at the mRNA level in CNS-purified mononuclear cells. The M1 (proinflammatory) activation markers TNFα and IL-1β were increased in CCRL2 KO mice at the peak of the disease (20 d.p.i.) and during the recovery phase (36 d.p.i.), whereas the M2 markers arginase and Ym1 were similarly expressed, with a clear decrease in arginase mRNA expression in CCRL2 KO cells observed only at 8 d.p.i. (**Fig. 7A**). Consistent with previous observations [31], immunohistochemistry performed at 16 and 33 d.p.i. detected the expression of the M2 marker Ym1 and the M1 marker IL-1β$^+$, in both WT and CCRL2 KO macrophages (Fig. 7B). Semiquantitative analysis was performed after normalization to Iba-1 staining. The number of M1-polarized macrophages was higher in CCRL2 KO than in WT mice at 16 and 33 d.p.i. (Fig. 7C). Conversely, M2 polarized macrophages were higher at the peak of the disease (16 d.p.i.) in WT mice, compared to CCRL2 KO mice and dramatically decreased at 33 d.p.i., suggesting that resolution of inflammation occurred in this group. On the contrary, at this later time (33 d.p.i.), in CCRL2 KO mice, M2 polarized macrophages were still numerous, indicating a delay in the recovery phase compared to that in WT animals. Microglia apparently did not acquire a significant expression of M1 and M2 polarization markers. These observations are consistent with the exacerbation of the disease observed in CCRL2 KO mice during the recovery phase (Fig. 2).

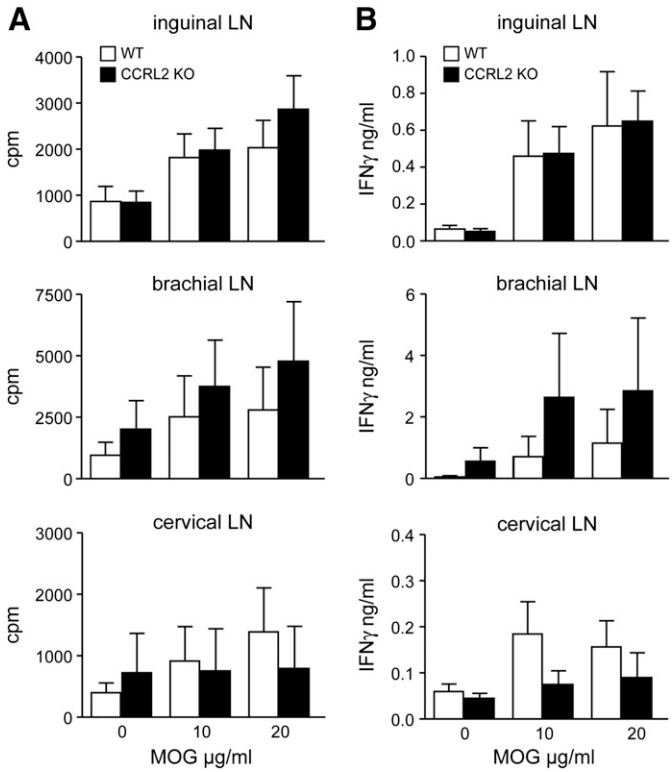


Figure 4. Antigen recall proliferation and IFNγ response are not impaired in CCRL2 KO lymph node–derived cells. Mice were immunized with $MOG_{aa35–55}$ emulsified in CFA. Ten days later, inguinal, brachial, and cervical draining lymph node cells were restimulated in vitro with the indicated concentrations of $MOG_{aa35–55}$. (A) After a 72 h stimulation, proliferation of lymph node cells was assessed by [^{3}H]-thymidine incorporation assay (cpm). The mean ± SEM of 5–6 mice per group is shown. (B) Culture supernatants were collected after 72 h stimulation, and levels of IFNγ were evaluated by ELISA. Data are representative of results in 2 independent experiments.

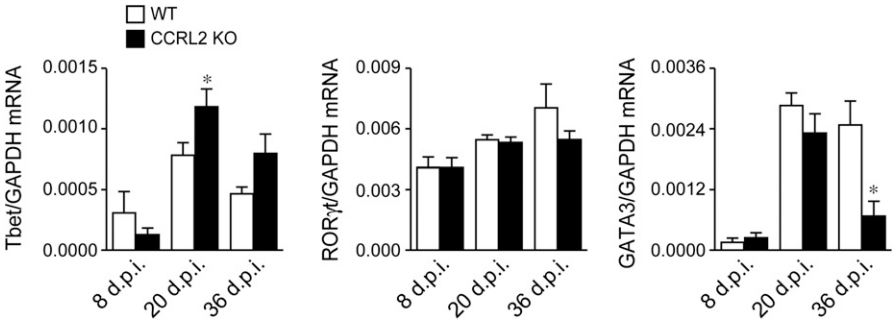


Figure 5. CNS T cell polarization is altered in CCRL2 KO mice during EAE. qRT-PCR analysis of mRNA expression of T cell-polarizing transcription factors, T-bet (Th1), RORγt (Th17), and GATA-3 (Th2), in CNS-infiltrating cells of $MOG_{aa35–55}$-immunized WT and CCRL2 KO mice at different time points (8, 20, and 36 d.p.i.). Data are means ± SEM of results in 5–6 mice per group. $^*P < 0.05$, WT vs. CCRL2 KO mice.

DISCUSSION

CCRL2 is a 7-transmembrane protein with structural and functional characteristics similar to the members of the "ACKR family." ACKRs are characterized by the lack of a highly conserved sequence in the third intracellular loop, known as the DRYLAIV motif, a motif that is relevant for G-protein coupling and activation of the signaling machinery. Therefore, these receptors are devoid of chemotactic functions. However, atypical chemotactic receptors undergo constitutive and ligand-induced scavenging and contribute to the control of inflammatory reactions by removing inflammatory ligands from inflamed tissues [6, 9].

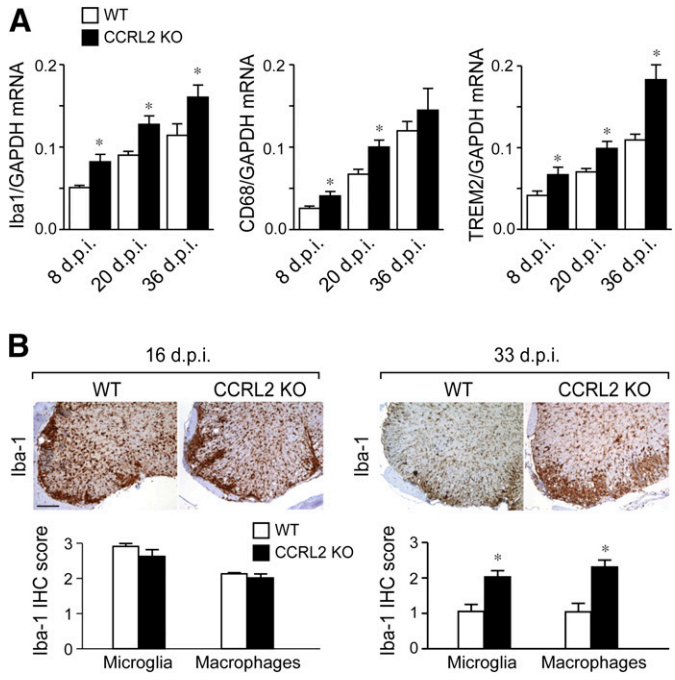


Figure 6. CCRL2 KO mice show increased microglia/macrophage activation markers during the EAE recovery phase. (A) Analysis of relative mRNA expression of the microglia/macrophage activation markers Iba-1, CD68, and TREM2 in CNS mononuclear cells obtained from $MOG_{aa35–55}$-immunized mice by qRT-PCR. Data are means ± SEM of results in 5–6 mice per group. (B) Representative sections of WT and CCRL2 KO spinal cords stained for Iba-1. Magnification, ×10. The lower bar graphs show microglia and macrophage activation in WT and CCRL2 KO spinal cords evaluated by a semiquantitative score of Iba-1 immunostaining and graded as follows: 0, none; 1, low; 2, moderate; and 3, high. $^*P < 0.05$, WT vs. CCRL2 KO mice.

CCRL2 maps at the edge of the main CCR cluster on chromosome 3 in a region of the genome where XCR1 and CCR1, -2, -3, and -5 are also located, and it exhibits high homology to CC chemokine receptors (about 40% amino acid identity with CCR1, -2, -3, and -5) [6, 9]. CCRL2 shows a ubiquitous expression in many leukocyte subsets, in astrocytes and in both lymphatic and hematic endothelial cells. Within leukocytes, CCRL2 is expressed by LPS-stimulated macrophages, neutrophils, mast cells, dendritic cells, and microglia and is upregulated in EAE [9, 19]. Studies performed in the past few years proposed CCRL2 as a receptor for some CC chemokines, such as CCL2, -5, -7, -8, and -19. However, the ability of CCRL2 to bind chemokines is still controversial (for a review see Ref. 9), and for this reason, CCRL2 has not yet been included in the recently proposed nomenclature for the ACKRs [6]. Similarly, the scavenging ability of CCRL2, an activity shared by ACKRs, needs further investigation [9]. CCRL2 binds chemerin, a chemotactic protein that also binds the functional chemotactic receptors ChemR23 and CCRL2 was proposed to function as a chemerin-presenting molecule [15]. In EAE, ChemR23 is expressed by activated microglia and by CNS-infiltrating dendritic cells. ChemR23 KO mice were shown to develop less severe EAE, and pharmacological inhibition of ChemR23 signaling reduced EAE severity [23, 32]. These findings clearly indicate that ChemR23 and chemerin are proinflammatory mediators in EAE.

We now report that, although CCRL2 shares the same ligand with ChemR23, CCRL2 KO mice were not only not protected, but exhibited exacerbated disease in an experimental model of EAE. This finding highlights a novel unexpected role for CCRL2 in the control of EAE-associated inflammation. The molecular mechanisms responsible for this effect are not fully understood. In our study, we failed to detect a defect in T cell priming during the immunization phase or a defect in the generation of Treg cells, a population known to be involved in EAE immune regulation [33].

Among the family of the ACKRs, ACKR3 has been shown to be upregulated and to play a role in EAE development. ACKR3 binds CXCL12, but in contrast to CXCR4, it does not transduce classic G-protein signaling, but rather removes the ligand from the extracellular milieu. ACKR3 contributes to the polarized expression of CXCL12 at the blood–brain barrier and restricts the entry of CXCR4-expressing T cells in the CNS [34]. Similar to the ACKR3-CXCL12 pair, both CCRL2 and chemerin, were upregulated in activated endothelial cells and in EAE in this study and others [17, 23], although the scavenging properties of CCRL2 are still controversial [15, 35]. Altogether, these findings

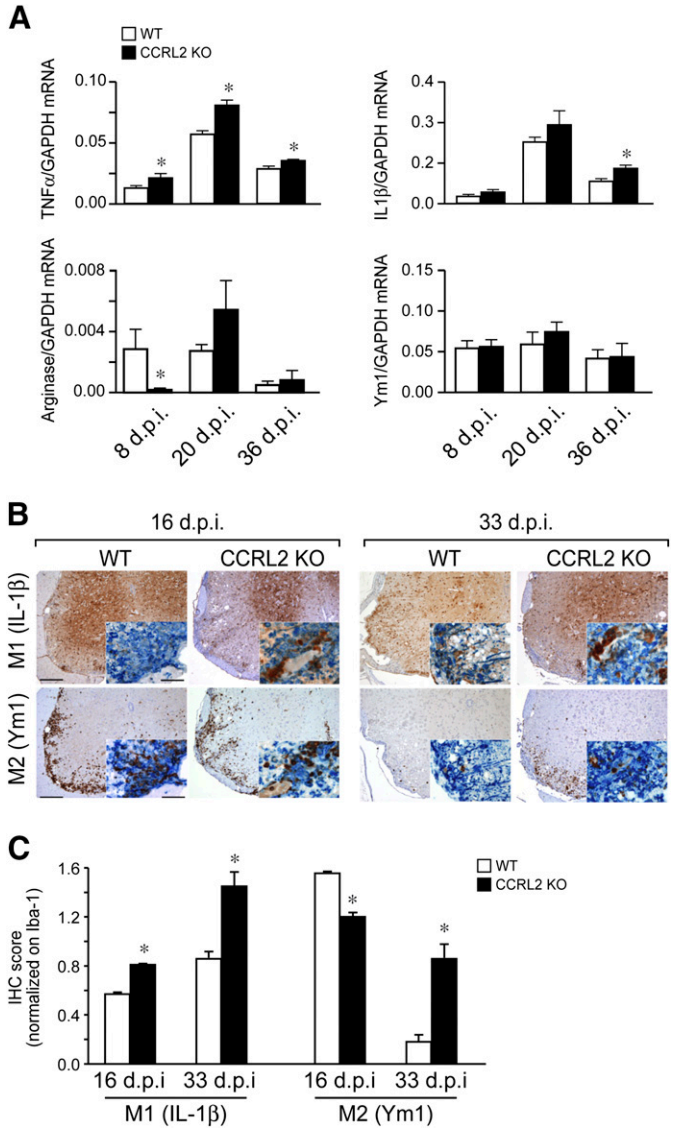


Figure 7. CCRL2 KO mice present an altered M1/M2 balance in CNS mononuclear cells during the EAE recovery phase. (A) Analysis of relative mRNA expression levels of M1- and M2-associated markers in CNS mononuclear cells obtained from $MOG_{aa35–55}$-immunized mice by qRT-PCR. Data are means ± SEM of results in 5–6 mice per group. (B) Representative sections of WT and CCRL2 KO spinal cords stained for a M1 (IL-1β)- and M2 (Ym1)-associated markers. Magnification, ×10 for single-stained and ×40 for double-stained sections. (C) Semiquantitative evaluation of macrophages expressing IL-1β (M1) or Ym1 (M2) markers, after normalization on Iba-1 staining. *$P < 0.05$, WT vs. CCRL2 KO mice.

suggest that CCRL2 plays a role in limiting the infiltration of ChemR23-expressing cells into the CNS. Alternatively, a new still undiscovered function of CCRL2 may be responsible for the increased inflammation and demyelination observed in CCRL2 KO mice. Further investigation is needed to fully investigate this question.

In autoimmune MS and in EAE, the development of demyelinating lesions within the CNS is associated with the perivascular accumulation of inflammatory mononuclear cells. Microglia and infiltrating macrophages can participate, in both the cytotoxic response and the resolution phase of inflammation, depending on their polarized activation state. Several studies have highlighted the importance of microglia in brain protection [28, 36]. Recently, a new molecule, TREM2, has been described as a regulator of microglia activation in the CNS [27, 30]. Our findings showing increased expression of TREM2 in CNS mononuclear cells, throughout the course of the disease, are in agreement with the exacerbated phenotype observed in CCRL2 KO mice. The acquisition of the M2 phenotype by resident microglia and by infiltrating macrophages is associated with neuroprotective properties and is an essential component of the CNS regenerative response [31, 36]. Our results show that the delayed EAE recovery phase observed in CCRL2 KO mice was associated with the defective acquisition of M2 markers by infiltrating macrophages, which resulted in an altered M1/M2 ratio that is likely responsible for the prolonged T cell perivascular infiltration and inflammatory reaction.

In summary, this study identified a novel function of CCRL2 in the control of EAE-associated inflammation. The evidence that CCRL2 plays a role in EAE makes this ACKR a candidate as a player and potential target in the control of inflammation in MS.

AUTHORSHIP

C.M., L.Z., L.W., V.S., and A.D.P. performed the experiments and contributed to analysis of the data and writing of the manuscript. E.F. and P.L.P. performed the histological analysis. S.S. contributed to the study concept and design and in drafting and revising the manuscript, including analysis and interpretation of data.

ACKNOWLEDGMENTS

This study was supported by Ministero dell'Istruzione Università e Ricerca (MIUR), Eurostar ChemExit Grant. 7306/8, and the Belgian Science Policy Office (Belspo). L.Z. is the recipient of a fellowship from "Fondazione Veronesi per la ricerca." The authors thank Cristina Ploia and Francesca Ruffini for technical help.

DISCLOSURE

The authors declare no conflicts of interest.

REFERENCES

1. Compston, A., Coles, A. (2008) Multiple sclerosis. *Lancet* **372,** 1502–1517.
2. Ransohoff, R. M. (2012) Animal models of multiple sclerosis: the good, the bad and the bottom line. *Nat. Neurosci.* **15,** 1074–1077.
3. Dendrou, C. A., Fugger, L., Friese, M. A. (2015) Immunopathology of multiple sclerosis. *Nat. Rev. Immunol.* **15,** 545–558.
4. Ajami, B., Bennett, J. L., Krieger, C., McNagny, K. M., Rossi, F. M. (2011) Infiltrating monocytes trigger EAE progression, but do not contribute to the resident microglia pool. *Nat. Neurosci.* **14,** 1142–1149.
5. Haghikia, A., Hohlfeld, R., Gold, R., Fugger, L. (2013) Therapies for multiple sclerosis: translational achievements and outstanding needs. *Trends Mol. Med.* **19,** 309–319.
6. Bachelerie, F., Ben-Baruch, A., Burkhardt, A. M., Combadiere, C., Farber, J. M., Graham, G. J., Horuk, R., Sparre-Ulrich, A. H., Locati, M., Luster, A. D., Mantovani, A., Matsushima, K., Murphy, P. M., Nibbs, R., Nomiyama, H., Power, C. A., Proudfoot, A. E., Rosenkilde, M. M., Rot, A.,

Sozzani, S., Thelen, M., Yoshie, O., Zlotnik, A. (2014) International Union of Basic and Clinical Pharmacology. [corrected]. LXXXIX. Update on the extended family of chemokine receptors and introducing a new nomenclature for atypical chemokine receptors. *Pharmacol. Rev.* **66,** 1–79.
7. Sozzani, S., Del Prete, A. (2015) Chemokines as relay signals in human dendritic cell migration: serum amyloid A kicks off chemotaxis. *Eur. J. Immunol.* **45,** 40–43.
8. Elhofy, A., Kennedy, K. J., Fife, B. T., Karpus, W. J. (2002) Regulation of experimental autoimmune encephalomyelitis by chemokines and chemokine receptors. *Immunol. Res.* **25,** 167–175.
9. Del Prete, A., Bonecchi, R., Vecchi, A., Mantovani, A., Sozzani, S. (2013) CCRL2, a fringe member of the atypical chemoattractant receptor family. *Eur. J. Immunol.* **43,** 1418–1422.
10. Cruz-Orengo, L., Chen, Y. J., Kim, J. H., Dorsey, D., Song, S. K., Klein, R. S. (2011) CXCR7 antagonism prevents axonal injury during experimental autoimmune encephalomyelitis as revealed by in vivo axial diffusivity. *J. Neuroinflammation* **8,** 170.
11. Shimada, T., Matsumoto, M., Tatsumi, Y., Kanamaru, A., Akira, S. (1998) A novel lipopolysaccharide inducible C-C chemokine receptor related gene in murine macrophages. *FEBS Lett.* **425,** 490–494.
12. Migeotte, I., Franssen, J. D., Goriely, S., Willems, F., Parmentier, M. (2002) Distribution and regulation of expression of the putative human chemokine receptor HCR in leukocyte populations. *Eur. J. Immunol.* **32,** 494–501.
13. Yoshimura, T., Oppenheim, J. J. (2011) Chemokine-like receptor 1 (CMKLR1) and chemokine (C-C motif) receptor-like 2 (CCRL2): two multifunctional receptors with unusual properties. *Exp. Cell Res.* **317,** 674–684.
14. Galligan, C. L., Matsuyama, W., Matsukawa, A., Mizuta, H., Hodge, D. R., Howard, O. M., Yoshimura, T. (2004) Up-regulated expression and activation of the orphan chemokine receptor, CCRL2, in rheumatoid arthritis. *Arthritis Rheum.* **50,** 1806–1814.
15. Zabel, B. A., Nakae, S., Zúñiga, L., Kim, J. Y., Ohyama, T., Alt, C., Pan, J., Suto, H., Soler, D., Allen, S. J., Handel, T. M., Song, C. H., Galli, S. J., Butcher, E. C. (2008) Mast cell-expressed orphan receptor CCRL2 binds chemerin and is required for optimal induction of IgE-mediated passive cutaneous anaphylaxis. *J. Exp. Med.* **205,** 2207–2220.
16. Monnier, J., Lewén, S., O'Hara, E., Huang, K., Tu, H., Butcher, E. C., Zabel, B. A. (2012) Expression, regulation, and function of atypical chemerin receptor CCRL2 on endothelial cells. *J. Immunol.* **189,** 956–967.
17. Gonzalvo-Feo, S., Del Prete, A., Pruenster, M., Salvi, V., Wang, L., Sironi, M., Bierschenk, S., Sperandio, M., Vecchi, A., Sozzani, S. (2014) Endothelial cell-derived chemerin promotes dendritic cell transmigration. *J. Immunol.* **192,** 2366–2373.
18. Zuurman, M. W., Heeroma, J., Brouwer, N., Boddeke, H. W., Biber, K. (2003) LPS-induced expression of a novel chemokine receptor (L-CCR) in mouse glial cells in vitro and in vivo. *Glia* **41,** 327–336.
19. Brouwer, N., Zuurman, M. W., Wei, T., Ransohoff, R. M., Boddeke, H. W., Biber, K. (2004) Induction of glial L-CCR mRNA expression in spinal cord and brain in experimental autoimmune encephalomyelitis. *Glia* **46,** 84–94.
20. Otero, K., Vecchi, A., Hirsch, E., Kearley, J., Vermi, W., Del Prete, A., Gonzalvo-Feo, S., Garlanda, C., Azzolino, O., Salogni, L., Lloyd, C. M., Facchetti, F., Mantovani, A., Sozzani, S. (2010) Nonredundant role of CCRL2 in lung dendritic cell trafficking. *Blood* **116,** 2942–2949.
21. Sozzani, S., Vermi, W., Del Prete, A., Facchetti, F. (2010) Trafficking properties of plasmacytoid dendritic cells in health and disease. *Trends Immunol.* **31,** 270–277.
22. Bondue, B., Wittamer, V., Parmentier, M. (2011) Chemerin and its receptors in leukocyte trafficking, inflammation and metabolism. *Cytokine Growth Factor Rev.* **22,** 331–338.
23. Graham, K. L., Zabel, B. A., Loghavi, S., Zuniga, L. A., Ho, P. P., Sobel, R. A., Butcher, E. C. (2009) Chemokine-like receptor-1 expression by central nervous system-infiltrating leukocytes and involvement in a model of autoimmune demyelinating disease. *J. Immunol.* **183,** 6717–6723.
24. Stromnes, I. M., Goverman, J. M. (2006) Active induction of experimental allergic encephalomyelitis. *Nat. Protoc.* **1,** 1810–1819.
25. Steinbach, K., McDonald, C. L., Reindl, M., Schweigreiter, R., Bandtlow, C., Martin, R. (2011) Nogo-receptors NgR1 and NgR2 do not mediate regulation of CD4 T helper responses and CNS repair in experimental autoimmune encephalomyelitis. *PLoS One* **6,** e26341.
26. Bosticardo, M., Musio, S., Fontana, E., Angiari, S., Draghici, E., Constantin, G., Poliani, P. L., Pedotti, R., Villa, A. (2014) Development of central nervous system autoimmunity is impaired in the absence of Wiskott-Aldrich syndrome protein. *PLoS One* **9,** e86942.
27. Poliani, P. L., Wang, Y., Fontana, E., Robinette, M. L., Yamanishi, Y., Gilfillan, S., Colonna, M. (2015) TREM2 sustains microglial expansion during aging and response to demyelination. *J. Clin. Invest.* **125,** 2161–2170.
28. Yamasaki, R., Lu, H., Butovsky, O., Ohno, N., Rietsch, A. M., Cialic, R., Wu, P. M., Doykan, C. E., Lin, J., Cotleur, A. C., Kidd, G., Zorlu, M. M., Sun, N., Hu, W., Liu, L., Lee, J. C., Taylor, S. E., Uehlein, L., Dixon, D., Gu, J., Floruta, C. M., Zhu, M., Charo, I. F., Weiner, H. L., Ransohoff, R. M. (2014) Differential roles of microglia and monocytes in the inflamed central nervous system. *J. Exp. Med.* **211,** 1533–1549.
29. Katsumoto, A., Lu, H., Miranda, A. S., Ransohoff, R. M. (2014) Ontogeny and functions of central nervous system macrophages. *J. Immunol.* **193,** 2615–2621.
30. Cantoni, C., Bollman, B., Licastro, D., Xie, M., Mikesell, R., Schmidt, R., Yuede, C. M., Galimberti, D., Olivecrona, G., Klein, R. S., Cross, A. H., Otero, K., Piccio, L. (2015) TREM2 regulates microglial cell activation in response to demyelination in vivo. *Acta Neuropathol.* **129,** 429–447.
31. Jiang, Z., Jiang, J. X., Zhang, G. X. (2014) Macrophages: a double-edged sword in experimental autoimmune encephalomyelitis. *Immunol. Lett.* **160,** 17–22.
32. Graham, K. L., Zhang, J. V., Lewén, S., Burke, T. M., Dang, T., Zoudilova, M., Sobel, R. A., Butcher, E. C., Zabel, B. A. (2014) A novel CMKLR1 small molecule antagonist suppresses CNS autoimmune inflammatory disease. *PLoS One* **9,** e112925.
33. Kohm, A. P., Carpentier, P. A., Anger, H. A., Miller, S. D. (2002) Cutting edge: CD4+CD25+ regulatory T cells suppress antigen-specific autoreactive immune responses and central nervous system inflammation during active experimental autoimmune encephalomyelitis. *J. Immunol.* **169,** 4712–4716.
34. Cruz-Orengo, L., Holman, D. W., Dorsey, D., Zhou, L., Zhang, P., Wright, M., McCandless, E. E., Patel, J. R., Luker, G. D., Littman, D. R., Russell, J. H., Klein, R. S. (2011) CXCR7 influences leukocyte entry into the CNS parenchyma by controlling abluminal CXCL12 abundance during autoimmunity. *J. Exp. Med.* **208,** 327–339.
35. Catusse, J., Leick, M., Groch, M., Clark, D. J., Buchner, M. V., Zirlik, K., Burger, M. (2010) Role of the atypical chemoattractant receptor CRAM in regulating CCL19 induced CCR7 responses in B-cell chronic lymphocytic leukemia. *Mol. Cancer* **9,** 297.
36. Liao, B., Zhao, W., Beers, D. R., Henkel, J. S., Appel, S. H. (2012) Transformation from a neuroprotective to a neurotoxic microglial phenotype in a mouse model of ALS. *Exp. Neurol.* **237,** 147–152.

KEY WORDS:
atypical chemokine receptors · chemokines · macrophages · microglia · inflammation · multiple sclerosis